http://doi.org/10.1109/JPHOTOV.2017.2666550

Cd and Cu interdiffusion in $Cu(In,Ga)Se_2$/CdS hetero-interfaces

P.M.P Salomé#, R. Ribeiro-Andrade, J.P. Teixeira, J. Keller, T. Törndahl, N. Nicoara, M. Edoff, J.C. González, J.P. Leitão, and S. Sadewasser

***Abstract*— We report a detailed characterization of an industry-like prepared $Cu(In,Ga)Se_2$ (CIGS)/CdS heterojunction by scanning transmission electron microscopy (STEM) and photoluminescence (PL). Energy dispersive x-ray spectroscopy (EDS) shows the presence of several regions in the CIGS layer that are Cu deprived and Cd enriched, suggesting the segregation of Cd-Se. Concurrently, the CdS layer shows Cd-deprived regions with the presence of Cu, suggesting a segregation of Cu-S. The two types of segregations are always found together, which, to the best of our knowledge, is observed for the first time. The results indicate that there is a diffusion process that replaces Cu with Cd in the CIGS layer and Cd with Cu in the CdS layer. Using a combinatorial approach we identified that this effect is independent of focused-ion beam sample preparation and of the TEM-grid. Furthermore, photoluminescence measurements before and after an HCl etch indicate a lower degree of defects in the post-etch sample, compatible with the segregates removal. We hypothesize that $Cu_{2-x}Se$ nanodomains react during the chemical bath process to form these segregates since the chemical reaction that dominates this process is thermodynamically favourable. These results provide important additional information about the formation of the CIGS/CdS interface.**

***Index Terms*—thin films, solar cells, $Cu(In,Ga)Se_2$ (CIGS), CdS, diffusion, Transmission electron microscopy (TEM).**

INTRODUCTION

$Cu(In,Ga)Se_2$ (CIGS) thin film solar cells have achieved remarkable values of power conversion efficiency mostly due to recent improvements in the CIGS/CdS interface formation via an alkali treatment [1],[2]. The CIGS/CdS hetero-interface has been the topic of many publications and as the post-deposition alkali surface treatment reveals, there are still open questions about its quality and distribution of elements. One of the open topics is the diffusion of Cd, S, and CdS into the CIGS layer and out-diffusion of elements from the CIGS layer into the CdS layer. Several conflicting reports are found in the literature, however, the exact diffusion mechanism is still being debated. This is likely due to the fact that the CIGS material and its electronic properties are highly dependent on the growth conditions. In any case, it has been well established that the diffusion of Cd into CIGS influences the electrical properties of the heterojunction. One of the most important findings of Cd influence was from Ramanathan *et al.*, who found that a Cd-electrolyte bath of the CIGS would provide Cd-free buffer solar cells with enhanced electrical performance when compared with non-treated ones [3]. The authors hypothesised that Cd was diffusing into the CIGS during the Cd-electrolyte treatment providing a beneficial effect. Lei *et al.*, have linked the electrolyte treatment to an increase of the charge carrier concentration and the lowering of the activation energy of the N1 defect [4]. This was supported by theoretical studies predicting lower surface recombination in devices with a Cd-doped CIGS surface [5]. Thus, an exact identification of the resulting interface is quite important. In addition to the diffusion of Cd into the CIGS, at least two other effects have been observed independently: i) Cu out-diffusion from the CIGS absorber during the CBD bath [6]-[12] and ii) the formation of Cd-Se bonds [13]-[18]. These observations have, so far, not been linked to any other effect.

In this work we study industry-like prepared CIGS/CdS interfaces using scanning transmission electron microscopy (STEM) and energy dispersive X-ray spectroscopy (EDS), a preferential technique to study local diffusion of elements due to its high spatial resolution. There are several other techniques that provide better composition sensitivity (secondary ion emission mass spectroscopy, X-ray photoelectron spectroscopy, etc.), but have lower spatial resolution and are therefore less suitable for this study. We report the presence of Cd-Se segregates in the CIGS layer and Cu-S segregates in the CdS layer. Photoluminescence (PL) measurements showed a strong influence of defects compatible with the above interdiffusion. The clear demonstration of this interdiffusion with unprecedented high spatial resolution brings upon a new understanding of the CIGS/CdS interface formation. Combinatorial experiments were designed to rule out any influence of the sample preparation and from the TEM-grid.

The authors acknowledge the Swedish Energy Agency (Grant no. 2012-004591), Sweden's innovation agency VINNOVA (Grant no.2013-02199), STandUP, CAPES (CAPES-INL 04/14), CNPq, FAPEMIG and the Portuguese Science and Technology Foundation (FCT) through the RECI-II/FIS-NAN/0183/2012 (COMPETE: FCOMP-01-0124-FEDER-027494) for funding.

P.M.P. Salomé, R. Ribeiro-Andrade, N. Nicoara, and S. Sadewasser are with the International Iberian Nanotechnology Laboratory (INL), Av. Mestre José Veiga, 4715-330 Braga, Portugal. J. Keller, T. Törndahl and M. Edoff are with the Ångström Solar Center, Solid State Electronics, Uppsala University, SE-75121 Uppsala, Sweden. J.P. Teixeira and J.P. Leitão are with Departamento de Física and I3N, Universidade de Aveiro, Campus Universitário de Santiago, 3810-193 Aveiro, Portugal. R-Ribeiro Andrade and J. C. González are with Departamento de Física, Universidade Federal de Minas Gerais, 30123-970 Belo Horizonte, Minas Gerais, Brasil.

#Corresponding author: P.M.P. Salomé – pedro.salome@inl.int

EXPERIMENTAL DESCRIPTION

A. Sample preparation

Solar cells with the structure soda-lime glass (SLG) /Mo/CIGS/CdS/i-ZnO/ZnO:Al/Ni-Al-Ni-grid were prepared using the Ångström solar cell baseline [19], which is based in semi-industrial methods. CIGS was prepared in an in-line evaporator using a one-stage co-evaporation process on 12.5×12.5 cm^2 substrates with an active evaporation time below 20 minutes [19],[20]. The CIGS composition is [Ga]/([In]+[Ga]) = 0.42 ± 0.03 and [Cu]/([In]+[Ga]) = 0.86 ± 0.03. 12 solar cells were fabricated with average light to power conversion efficiency around 15 %. For the characterizations that needed non-finished solar cells, i.e. SLG/Mo/CIGS/CdS, pieces of the sample were used where the processing finished right after the CdS deposition. To prevent any possible degradation of the materials, storage, transport, and shipping of all samples between growth and characterization, were made either in low-vacuum, or in a dry N_2 environment.

B. TEM characterization

STEM images were taken with a FEI Titan ChemiStem 80-200 kV Cs-probe corrected TEM, operating at 200 kV accelerating voltage and equipped with an EDS SuperX Bruker detector. In this method a coherent focused probe scans across the specimen and the X-ray emission spectrum is recorded in each probe position. All samples studied in cross section mode were prepared in a focused ion beam (FIB) FEI Dual-Beam Helios 450S with FIB lift-out Cu- or Mo [21]. In all of the samples a layer of amorphous carbon was deposited to reduce shadowing effects and to improve the electrical conductivity of the surface. On top of the buffer layer a protective Pt bi-layer assisted by the electron and the Ga beam was deposited. The lamellae were prepared as thin as possible, < 150 nm for 30KV and <50nm for 1KV.

In order to validate the findings of this work we need to rule out three possible artefacts: 1) morphological and compositional modifications to the cross-section generated during the FIB final polishing process [22]; 2) shadowing effect of the lamella cutting also during the FIB preparation; and 3) superimposition in the EDS quantification of specimen elements with elements from the TEM grid or the FIB preparation process. Several lamellae were prepared as shown in Table I. Different samples, i.e. CIGS/CdS or complete solar cells were used to confirm that no shadowing, or curtain effects, are influencing our results. Since effects connected with the interaction of the polishing beam with the specimen will be connected with the polishing ion-energy, two different Ga final polishing energies were studied: 1 keV and 30 keV. By changing the TEM grid material, EDS superimposition problems connected with elemental identification were avoided. By using a Cu TEM grid, the identification of Cu in the specimen might be questionable, whereas with the Mo TEM grid there is a superimposition of the Mo-$L_{\alpha 1}$ (2.293 keV) and the S-$K_{\alpha 1}$ (2.307 keV) lines. However, in the case of Mo, we also measured the Mo-$K_{\alpha 1}$ to discriminate the Mo and S signal. Thus, the combination of using both grids can reduce, or possibly remove potential errors. Furthermore, since the FIB polishing is done with a Ga^+ beam, special care has to be taken when looking at the Ga counts. By taking the number of counts for Ga in the electron beam induced deposited Pt layer (Pt-EBID) and subtracting this value from the Ga signal a good approximation of the Ga signal coming from the sample could be obtained. For the measurements that were performed using a Cu grid, there is a residual emission observable for Cu throughout the whole lamella that can be also subtracted from the Cu signal in the Pt layer. The Cd-$L_{\alpha 1}$ line (3.133 keV) has no superimpositions and can be easily analysed. For In there is a superimposition of the In-$L_{\alpha 1}$ line (3.287 kev) with the Cd-$L_{\beta 1}$ (3.316 keV). A possible way to distinguish both elements would be to look for the K_α lines of Cd (23.106 keV) and In (24.136 keV) which do not overlap, however their intensities are low. Another way to account for In is to calculate [(In-$L_{\alpha 1}$) - (Cd-$L_{\alpha 1}$)] instead of only looking for In-L_α. Although this method has limited physical meaning, the similarity between [(In-$L_{\alpha 1}$) - (Cd-$L_{\alpha 1}$)] and In-K_α indicates the validity of this method and thus we can evaluate where In is located. Images taken before and after performing the EDS mapping and linescan showed no damage from the beam.

C. Photoluminescence

The photoluminescence (PL) measurements were carried out using a Bruker IFS 66v Fourier transform infrared (FTIR) spectrometer equipped with a Ge diode detector. The samples were inserted in a helium gas flow cryostat which allows for measurements at 5 K. The excitation source was the 514.5 nm line of an Ar^+ ion laser, with the laser power measured at the front of the cryostat window with an area of a few mm^2. The PL spectra were corrected for the sensitivity of the Ge detector.

RESULTS

A. Transmission electron microscopy

A total of 6 lamellae were prepared according to the conditions described in Table I. All of the samples show the same features. Since the lamellae were prepared in different conditions and all show the features that we are analysing, a combinatorial analysis allows us to discard several effects. By comparing samples A-B, which do not have the window layers, with samples C-F we can discard curtain effects from the FIB preparation process. By comparing samples A, C, and E, which were prepared by using a FIB last polishing step of 1 kV, with samples B, D, and F, which were prepared by using a FIB last polishing step of 30 kV, we can conclude that the FIB preparation is not influencing our results. Finally by comparing samples A-D, which were prepared using a Mo grid, to samples E and F, which were prepared with a Cu grid, we can discard any EDS superimposition problem between the sample and the grid elements. For simplicity purposes we will only show EDS results for sample C and sample E.

TABLE I
TEM LAMELLAE OF DIFFERENT SAMPLES WITH FINAL GA ACCELERATION VOLTAGE POLISHING AND DIFFERENT TEM GRIDS USED.

Sample	Final Polishing	TEM grid material
A - CIGS/CdS	1 kV	Mo
B - CIGS/CdS	30 kV	Mo
C - carbon coated–full solar cell	1 kV	Mo
D - carbon coated–full solar cell	30 kV	Mo
E - carbon coated–full solar cell	1 kV	Cu
F - carbon coated–full solar cell	30 kV	Cu

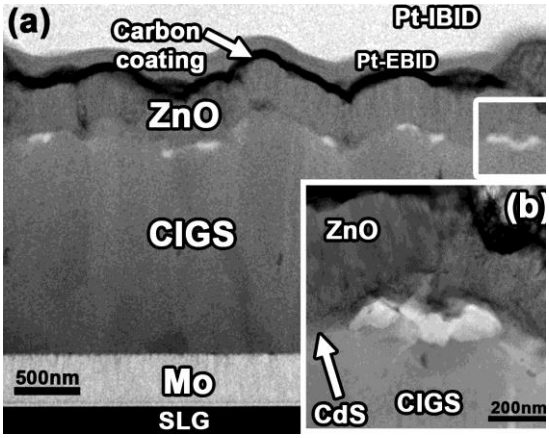

Fig. 1. (a) HAADF image of the prepared lamella of sample D showing the CIGS/CdS heterojunction. (b) Shows a detail of this interface.

Fig. 1 shows a high-angle annular dark field (HAADF) image of sample D showing the CIGS/CdS/ZnO/carbon/Pt layer stack. Fig. 1 (b) shows a close up of the CIGS/CdS interface. Even though in Fig. 1 (a) the CdS layer appears conformal and uniform, its uniformity is not perfect, since there are a small number of regions where the morphology is slightly different, as seen in Fig. 1 (b). These small regions are 10-400 nm in length and they were found in all lamellae in a density of ~1/µm (2-3 regions per lamella and the lamella has a length of ~2.5 µm). Fig. 2 shows the bright field (BF) image, the EDS line profiles, and mapping of Cu, Cd, S, and Se of such regions for sample C. The EDS line profiles show the CIGS (left side) and the CdS (right side). We observe that between 0 nm and 140 nm, the counts of Cu, In, and Ga lower gradually until 140 nm at what appears to be the interface, since the Se counts drop sharply and the S counts increase. The Se counts are flat while the Cd counts exhibit a gradient with a high value at the interface, which decreases going towards the bulk of the CIGS. The shape of these profiles hints to a diffusion profile of Cd and to the formation of a Cd-Se segregate, since there is a region between 100 to 130 nm where there is only Cd and Se present. It is worth pointing out that at the position where the S signal increases, between 130 to 170 nm, the Cu counts also increase.

Fig 3 shows the analysis for sample E. In this case we see a more defined segregate of Cd-Se below a segregation of Cu-S. Such effect can be seen in the rectangular region at the bottom of the bright field image, where the EDS linescan measurements were performed. Both analyses are representative of several regions found in all the prepared lamellae, indicating that there are CIGS regions deficient of Cu, In, and Ga, but that surprisingly contain Cd. Concurrently, right on top of the Cd-Se rich regions, we identified a region on the CdS side that lacks Cd and that contains Cu and S. Outside these regions, the interface shows abrupt elemental transitions. Thus, most of the CIGS/CdS interface is well defined, but there are small regions where segregates of Cd-Se can be found inside of what should be CIGS and Cu-S segregates inside of what should be CdS, which is the first time such observation is made. Using XPS, several reports have shown Cd bound to Se [16]-[18], in agreement with our finding. However, here we clearly show that the Cd-Se segregate is spatially localized and not a surface layer as was hypothesised.

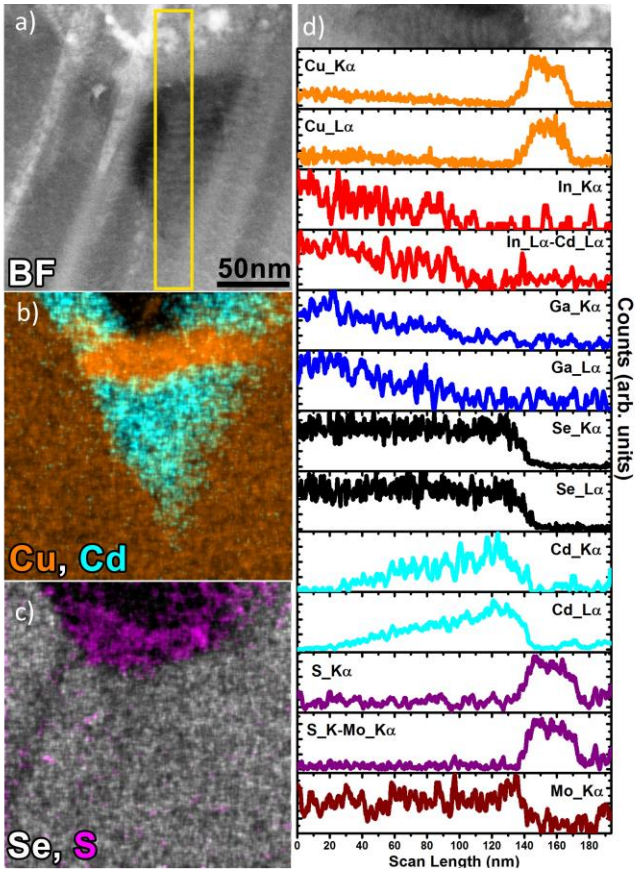

Fig 2. EDS analysis of sample C. (a) BF image. The rectangle indicates the line profiles region. (b) EDS mappings of Cu and Cd and (c) of Se and S. (d) EDS line profiles for all elements for several emission lines.

B. Photoluminescence

In order to investigate the influence of elemental diffusion into the CIGS on their optoelectronic properties, PL studies on the CIGS/CdS hetero-interface were performed. Subsequently, the sample was wet etched by using a 10% HCl solution (it is known that HCl etches CdS and Cu-Se compounds [23]) followed by another PL measurement. With the excitation wavelength of 514.5 nm, the observed emission should come from a superficial layer on the CIGS with a thickness of ~70 nm, according to the optical absorption data from [24]. We note that the layer scrutinized by the PL is where the segregates were detected. Thus, we can evaluate the effect of the segregates on

the CIGS hetero-interface by comparing the two PL measurements.

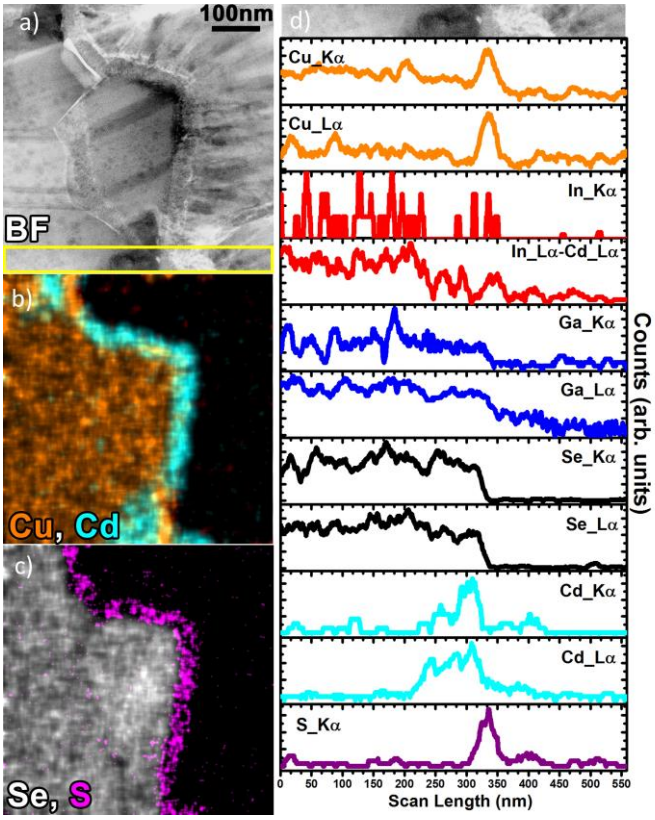

Fig 3. EDS analysis of sample E. (a) BF image. The rectangle indicates the line profiles region. (b) EDS mappings of Cu and Cd and (c) of Se and S. (d) EDS line profiles for all elements for several emission lines.

The normalised PL spectra measured for the same excitation power (10 mW) at 5 K, before and ~10 minutes after the etching, are shown in Fig. 4 (a). Each spectrum is presented with its own energy scale, such that the peak positions overlap. In that way, it is easily seen that after the etching, the emission narrows and clearly has a less asymmetric shape. The shape change is more pronounced on the low energy side of the emission. Additionally, the dependence of the peak position with the excitation power [25] was investigated and a blueshift of 13.5 ± 0.2 meV/decade was estimated for the measurements with the CdS layer and 11.7 ± 0.5 meV/decade for the measurements after the etching. We note that this type of emission in chalcopyrite materials is usually associated with electrostatic fluctuating potentials [26]-[29].

Another approach to compare the influence of electrostatic fluctuating potentials in the two samples is based on the analysis of the emission in the low energy side [30-33]. For sufficiently deep states, the intensity in the low energy side of the emission, follows a Gaussian distribution. Moreover, the intensity of the emission in the low energy side, $I\ (h\nu)$, follows the density of states of the valence band tail [30-32]:

$$I\ (h\nu) \propto \frac{1}{\gamma}\exp\left(-\frac{\left(E_g - E_I - h\nu\right)^2}{2\gamma^2}\right) \quad (1)$$

where E_g is the band gap energy of the doped semiconductor, E_I is the binding energy of the hole to an acceptor level and γ describes the root mean square depth of the potential wells in the valence band. We obtained γ values of 39.6 $\pm$ 0.1 meV and 35.2 $\pm$ 0.4 meV for the sample with before and after the etching, respectively. The reduction of γ supports the reduction of the asymmetry of the band (Fig 4(a)) and the results obtained by the power dependence. These findings suggest that after performing the chemical etching, the CIGS is less affected by electrostatic fluctuating potentials. This type of fluctuating potentials in the electronic structure is created by interactions of ionised defects and dominate the radiative recombination channels when a high doping and strong compensation occurs. Thus, the luminescence reflects a likely change in the density of those defects. A significant contribution to these defects can originate from the CIGS surface since the defects on that layer should have a relevant impact in the PL emission [33]. Therefore, the lowering of the defect density seen by PL, allows us to assume that when the sample is etched, a fraction of ionised defects, like for instance CIGS/segregates interface traps, are removed. Therefore, the PL analysis supports the TEM results and provides further evidence for the influence of these segregates on the opto-electronic CIGS properties.

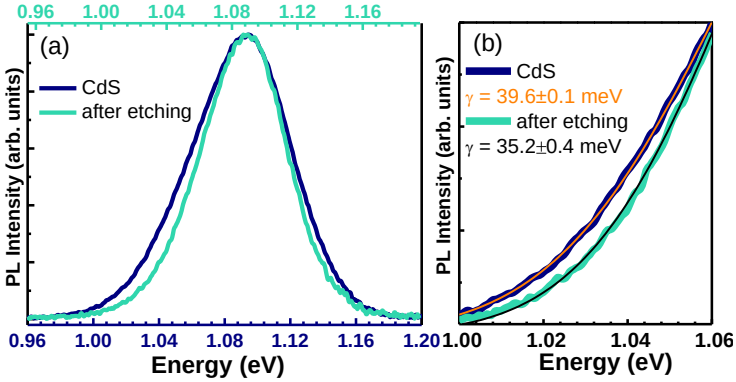

Fig.4: (a) Comparison of the normalised PL before and after the HCl etching, at 5 K and excitation power of 10 mW. The energy scale before and after the etch are the bottom and upper axis, respectively. (b) Low-energy side of the normalised PL fitted with Eq. (1) with the same axis and showing values of γ.

RELATION WITH THE LITERATURE AND DISCUSSION OF RESULTS

Already in 1999, Nakada et al. used TEM to observe the presence of Cd in the CIGS layer and a decrease of the Cu signal at the CIGS surface. The authors concluded that Cu was being replaced by Cd ions [5],[7] and pointed out that their ionic radii, 0.97 Å for Cd^{2+} and 0.96 Å for Cu^{+}, are very similar thereby favouring an interchange of the two atoms. However, these papers did not report modifications to the CdS layer. Using angle resolved X-ray photoelectron spectroscopy (ARPES), Liao et al. reported that only the first couple of atomic layers of epitaxial $CuInSe_2$ were heavily doped with Cd [8],[9], but not the rest of the bulk sample. The diffusion of Cd into the CIGS has been validated by several other groups using different techniques [10],[34],[35]. Concerning the Cu diffusion from the CIGS into the CdS layer, Abou-Ras *et al.* showed preliminary results of Cu diffusion from the CIGS into the CdS layer [36]. In addition, a Cd enrichment of the CIGS was also shown but their results were not completely clear due to the limited spatial resolution available at that time in conventional TEM and it is unclear if such effect was present in the whole surface or if it was localized in some regions. Diffusion of Cu into the CdS layer and diffusion of Cd into the absorber has been observed

for Cu-rich $CuGaSe_2$ and using a chemical bath deposition (CBD) at 80 ºC [13]. In spite of the very different absorber layer in comparison to the present work, such identification was also performed with XPS which, again, ruled out the possibility to identify if such effect was present in the whole surface or if it was a localized effect. Diffusion of Cd and S into the CIGS along the grain boundaries (GBs) of the CIGS has been reported by Rusu *et al*. [37]. Similar TEM results as the ones presented in this paper for CIGS and CBD-CdS were found by Park *et al*. [15], however their analysis was performed on samples that were annealed at temperatures above 200 ºC. Additionally, Lei *et al*., also using TEM, have observed the presence of Cu in the CdS layer, but have only seen CdS present at the GBs of the CIGS [4]. Although it has been shown that Cd diffuses in the CIGS mostly in the bulk and not in the GBs [34], a theoretical study has shown that the most likely diffusion mechanism is based on two steps by creating a Cu vacancy in the CIGS followed by a displacement of Cd into the vacancy [38]. These processes have energy barriers of 1 eV and 0.5 eV, respectively [38], in accordance with experimental data [34].

Even though several effects have been observed independently in previous studies, our results provide for the first time a complete picture of the interdiffusion occurring at the CIGS/CdS interface in CIGS material fabricated by an industry-relevant process. Nevertheless, the exact mechanism for the segregation and diffusion behaviour is yet to be identified. Our combinatorial approach for the preparation and use of TEM grids provides a high degree of reliability that the segregates are real since every lamella displayed the segregates. The combined TEM-EDS studies show segregation is not creating a thin layer but is spatially localised in the form of nanodomains. Furthermore, the PL measurements show that by chemically etching the samples, the concentration of ionised defects is reduced, something that is compatible with a lowering of the number of non-native elements in the CIGS.

A possibility for the appearance of both segregates identified in this work could be through the condensation of Se at the surface of the CIGS. This can occur during the cool-down phase after the growth of the CIGS [39] and would explain areas of the CIGS that are free of In and Ga but rich in Se. However, why this situation would promote a Cu-Cd interfusion is not understood. However, solar cells where Se condensation is reported, typically show decreased quantum efficiency behaviour around the bandgap of crystalline Se (~1.7 eV), which is not the case here. Therefore, we consider the condensation of crystalline Se in the present samples unlikely.

Even though the CIGS present in this work is Cu-poor and far from stoichiometry, we note that nano-sized Cu-rich and Cu-poor areas have been found by TEM analyses on Cu-poor CIGS [40]. It is also known that there is Cu-leaching from the CIGS film during the CdS-CBD [41]. Thus, a possible explanation for the results presented here is that prior to the CdS-CBD there are regions of the film with $Cu_{2-x}Se$ phases present and that in the presence of the strong basic solution of the CBD the following reaction may take place [15]:

$$Cu_{2-x}Se + CdS \rightarrow Cu_{2-x}S + CdSe \qquad (2)$$

The presence of Cd-Se bonds has been identified before using XPS for Cu-rich $CuGaSe_2$ [13]. Even though that study has not shown segregations, it has only shown the bonds, the presence of the Cd-Se bounds has been linked to variations in the CBD processing [13]. In addition, this reaction is thermodynamically favourable due to its reaction free energy of -5.6 kJ/mol, requiring only that the CIGS film has some aggregates of Cu_2Se [42]. $Cu_{2-x}S$ phases are highly conductive and could be detrimental for solar cell performance when present in the CdS due to shunts. The identification of $Cu_{2-x}S$ segregates in the CdS has also been shown for physical vapour deposited CdS [43,44] indicating its formation is not unique to the CdS-CBD process.

CONCLUSION

Using STEM we identified several regions of the CIGS/CdS interface where an inter-diffusion of Cu and Cd is observed. In these regions the CIGS area shows segregates consisting of Cd-Se, whereas the CdS layer shows segregates of Cu-S. We show for the first time that these regions always appear together. The results suggest that Cu takes the place of Cd in the CdS layer. To ensure that potential artefacts from the FIB sample preparation and from the STEM measurements can be ruled out, several TEM lamellae were prepared and results were compared in a combinatorial approach. We concluded that the segregates are present independently of the FIB preparation methods. The presence of Cu in the CdS layer is important since Cu may act as a doping element in CdS and in the extreme case $Cu_{2-x}S$ can form, which can be potentially harmful for the electrical performance of the solar cells.

Photoluminescence measurements show that by performing a wet etching that removes the segregates, the PL emission of the CIGS is affected by a smaller density of ionised defects. Such fact is in agreement with the segregates influencing the CIGS opto-electronic properties. The segregates can potentially create defects at the CIGS surface and thereby the PL analysis validates the TEM results.

We suggest that nanodomains of $Cu_{2-x}Se$ present on the CIGS layer react with the CdS from the CBD to form segregates of Cd-Se on the CIGS layer and to form Cu-S segregates in the CdS layer. Such mechanism can be explained by a thermodynamically favourable chemical process and is a good indication why we detect the segregates together. The findings in this work might not be universal for every CIGS layer since different CIGS compositions and different deposition recipes have a great influence in the properties of the resulting junction. Nevertheless, the layers used in the present study are highly relevant as they were prepared with a semi-industrial process that gives high-performance solar cells.

REFERENCES

[1] P. Reinhard, F. Pianezzi, B. Bissig, A. Chirila, P. Blösch, S. Nishiwaki, S. Buecheler, and A. N. Tiwari, *Cu(In,Ga)Se_2 Thin-Film Solar Cells and Modules— A Boost in Efficiency Due to Potassium*, IEEE Journal of Photovoltaics, vol. 5, no. 2, pp. 656-663, 2015.

[2] P. Jackson, R. Wuerz, D. Hariskos, E. Lotter, W. Witte, M. Powalla, *Effects of heavy alkali elements in Cu(In,Ga)Se_2 solar cells with efficiencies up to 22.6%*, Phys. Status Solidi RRL, vol.10, pp.583-586, 2016.

[3] K. Ramanathan, F. S. Hasoon, S. Smith, D. L. Young, M. A. Contreras, P. K. Johnson, A. O. Pudov, J. R. Sites, *Surface treatment of $CuInGaSe_2$ thin films and its effect on the photovoltaic properties of solar cells*, Journal of Physics and Chemistry of Solids, vol. 64, pp. 1495–1498, 2003.

[4] B. Lei, W. W. Hou, S.-H. Li, W. Yang, C.-H. Chung, and Y. Yang, *Cadmium ion soaking treatment for solution processed $CuInS_xSe_{2-x}$ solar cells and its effects on defect properties*, Solar Energy Materials & Solar Cells, vol.95, pp. 2384–2389, 2011.

[5] B. Yin, and C. Lou, *(112) Surface of $CuInSe_2$ Thin Films with Doped Cd Atoms*, Advances in Condensed Matter Physics, vol. 2015, 206501, 7 pp.

[6] T. Nakada, and A. Kunioka, *Direct evidence of Cd diffusion into $Cu(In,Ga)Se_2$ thin films during chemical-bath deposition process of CdS films*, Applied Physics Letters, vol. 74, pp. 2444-2446, 1999.

[7] T. Nakada, *Nano-structural investigations on Cd-doping into $Cu(In,Ga)Se_2$ thin films by chemical bath deposition process*, Thin Solid Films, vols. 361-362, pp. 346-352, 2000.

[8] D. Liao, and A. Rockett, *Cu depletion at the $CuInSe_2$ surface*, Applied Physics Letters, vol. 82, pp. 2829-2831, 2003.

[9] D. Liao, and A. Rockett, *Cd doping at the $CuInSe_2$ CdS heterojunction*,"Journal of Applied Physics, vol. 93, pp. 9380-9382, 2003.

[10] O. Cojocaru-Mirédin, P. Choi, R. Wuerz, and D. Raabe, *Atomic-scale characterization of the $CdS/CuInSe_2$ interface in thin-film solar cells*, Applied Physics Letters, vol. 98, pp. 103504-1-103504-3, 2011.

[11] D. Abou-Ras, G. Kostorz, A. Romeo, D. Rudmann, and A. N. Tiwari, *Structural and chemical investigations of CBD- and PVD-CdS buffer layers and interfaces in $Cu(In,Ga)Se_2$-based thin film solar cells*, Thin Solid Films, vols. 480–481 , pp.118– 123, 2005.

[12] C. Lei, M. Duch, I. M. Robertson, and A. Rockett, *Effects of solution-grown CdS on $Cu(In,Ga)Se_2$ grain boundaries*, Journal of Applied Physics, vol. 108, pp. 114908-1-114908-7, 2010.

[13] V. Nadenau, D. Hariskos, H.-W. Schock, M. Krejci, F.-J. Haug, A. N. Tiwari, H. Zogg, and G. Kostorz, *Microstructural study of the $CdS/CuGaSe_2$ interfacial region in $CuGaSe_2$ thin film solar cells*, Journal of Applied Physics, vol. 85, pp. 534-542, 1999.

[14] C. Heske, D. Eich, R. Fink, E. Umbach, T. van Buuren, C. Bostedt, L J. Terminello, S .Kakar, M. M. Grush, T. A. Callcott, F. J. Himpsel, D. L. Ederer, R. C. Perera, W. Riedl, and F. Karg, *Observation of intermixing at the buried $CdS/Cu(In,Ga)Se_2$ thin film solar cell heterojunction*, Applied Physics Letters, vol. 74, pp. 1451-1453 ,1999.

[15] S.-Y. Park, E.-W. Lee, S.-H. Lee, S.-W. Park, W. K. Kim, S. H. Lee, W.-G. Lee, B. J. Lee, H. K. Bae, J. H. Yoo, and C.-W. Jeon, *Investigation of $ZnO/CdS/CuIn_xGa_{1-x}Se_2$ interface reaction by using hot-stage TEM*, Current Applied Physics, vol. 10, pp. S399–S401, 2010.

[16] I. Luck, U. Störkel, W. Bohne, A. Ennaoui, M. Schmidt, H.W. Schock, and D. Bräunig, *Influence of buffer layer and TCO deposition on the bulk properties of chalcopyrites*, Thin Solid Films, vol. 387, pp.100-103, 2001.

[17] S. Pookpanratana, I. Repins, M. Bär, L. Weinhardt, Y. Zhang, R. Félix, M. Blum, W. Yang, and C. Heske, *$CdS/Cu(In,Ga)Se_2$ interface formation in high-efficiency thin film solar cells*, Applied Physics Letters, vol. 97, pp. 074101-1-074101-3, 2010.

[18] J.-F. Han, C. Liao, L.-M. Cha, T. Jiang, H.-M. Xie, K. Zhao, and M.-P. Besland, *TEM and XPS studies on CdS/CIGS interfaces*, Journal of Physics and Chemistry of Solids, vol. 75, pp.1279–1283, 2014.

[19] J. Lindahl, U. Zimmermann, P. Szaniawski, T. Törndahl, A. Hultqvist, P. M. P. Salomé, C. Platzer-Björkman, and M. Edoff, *In-line $Cu(In,Ga)Se_2$ Co-evaporation for High Efficiency Solar Cells and Modules*, IEEE Journal of Photovoltaics, vol. 3, no. 3, pp.1100-1105, 2013.

[20] P. M. P. Salomé, V. Fjällström, P. Szaniawski, J.P. Leitão, A. Hultqvist, P. A. Fernandes, J. P. Teixeira, B. P. Falcão, U. Zimmermann, A. F. da Cunha, and M. Edoff, *A comparison between thin film solar cells made from co-evaporated $CuIn_{1-x}Ga_xSe_2$ using a one-stage process versus a three-stage process*, Progress in Photovoltaics: Research and Applications, vol. 23, pp. 470–478, 2015.

[21] S. Bals, W. Tirry, R. Geurts, Z. Yang, and D. Schryvers, "*High-quality sample preparation by low kV FIB thinning for analytical TEM measurements*," Microscopy and Microanalysis, vol. 13, pp. 80-86, 2007.

[22] J. Y. Lee, W. K. Seong, M. Joe, K.-R. Lee, J.-K. Park, M.-W. Moon, and C.-W. Yang, *In-situ observation of ion beam-induced nanostructure formation on a $Cu(In,Ga)Se_2$ Surface*, Surface and Interface Analysis, vol. 44, pp. 1542–1546, 2012.

[23] W. Guo, J. J. Li, Y. A. Wang, and X. Peng, *Luminescent CdSe/CdS Core/Shell Nanocrystals in Dendron Boxes: Superior Chemical, Photochemical and Thermal Stability*, Journal of the American Chemical Society, vol. 125, pp. 3901-3909, 2003.

[24] P. D. Paulson, R. W. Birkmire, and W. N. Shafarman, *Optical characterization of $CuIn_{1-x}Ga_xSe_2$ alloy thin films by spectroscopicellipsometry*, J. Appl. Phys., Vol. 94, No. 2, 15 July 2003

[25] P.M.P. Salomé, J. Keller, T. Törndahl, J.P. Teixeira, N. Nicoara, R.-Ribeiro Andrade, D.G. Stroppa, J.C. González, M. Edoff, J.P. Leitão, S. Sadewasser, *CdS and $Zn_{1-x}Sn_xO_y$ buffer layers for CIGS solar cells*, Solar Energy Materials & Solar Cells 159, pp. 272–281, 2017.

[26] Distorter, D. M. Hofmann, D. Meister, B. K. Meyer, W. Riedl, and F. Karg, *Postgrowth thermal treatment of $CuIn(Ga)Se_2$: Characterization of doping levels in In-rich thin films*, Journal of Applied Physics, vol. 85, pp. 1423-1428, 1999.

[27] S. A. Schumacher, J. R. Botha, and V. Alberts, Photoluminescence study of potential fluctuations in thin layers of $Cu(In_{0.75}Ga_{0.25})(S_ySe_{1-y})_2$," Journal of Applied Physics, vol. 99, pp.063508-1- 063508-8, 2006.

[28] M. J. Romero, H. Du, G. Teeter, Y. Yan, M. M. Al-Jassim, *Comparative study of the luminescence and intrinsic point defects in the kesterite Cu_2ZnSnS_4 and chalcopyrite $Cu(In,Ga)Se_2$ thin films used in photovoltaic applications*," Physical Review B, vol. 84, pp.165324-1-165324-5, 2011.

[29] J. P. Teixeira, R. A. Sousa, M. G. Sousa, A. F. da Cunha, P. A. Fernandes, P. M. P. Salomé, J. C. González, J. P. Leitão, *Comparison of fluctuating potentials and DAP transitions in a Cu-poor Cu_2ZnSnS_4 based solar cell*, Applied Physics Letters, vol. 105, pp.163901-1-163901-4, 2014.

[30] A. P. Levanyuk and V. V. Osipov, Edge luminescence of direct-gap semiconductorsSov. Phys. Usp., vol. 24, p. 187, 1981.

[31] S. A. Jensen, S. Glynn, A. Kanevce, P. Dippo, J. V. Li, D. H. Levi and D. Kuciauskas, *Beneficial effect of post-deposition treatment in high-efficiency $Cu(In,Ga)Se_2$ solar cells through reduced potential fluctuations*, J. Appl. Phys 120, 063106, 2016.

[32] John K. Katahara and Hugh W. Hillhouse, Quasi-Fermi level splitting and sub-bandgap absorptivity from semiconductor photoluminescence; J. Appl. Phys. 116, 173504, 2014.

[33] A. Hultqvist, J. V. Li, D. Kuciauskas, P. Dippo, M. A. Contreras, D. H. Levi, and S. F. Bent, *Reducing interface recombination for $Cu(In,Ga)Se_2$ by atomic layer deposited buffer layers*, Applied Physics Letters, vol. 107, pp. 033906-1-033906-5, 2015.

[34] N. J. Biderman, Steven W. Novak, R. Sundaramoorthy, Pradeep Haldar, and J. R. Lloyd, "*Insights into cadmium diffusion mechanisms in two-stage diffusion profiles in solar grade $Cu(In,Ga)Se_2$ thin films*," Applied Physics Letters, vol. 107, pp. 232104-1- 232104-4, 2015.

[35] K. Hiepko, J. Bastek, R. Schlesiger, G. Schmitz, R. Wuerz, and N. A. Stolwijk, *Diffusion and incorporation of Cd in solar-grade $Cu(In,Ga)Se_2$ layers*, Applied Physics Letters, vol. 99, pp. 234101-1-234101-3, 2011.

[36] D. Abou-Ras, G. Kostorz, A. Romeo, D. Rudmann, A. N. Tiwari, *Structural and chemical investigations of CBD- and PVD-CdS buffer layers and interfaces in $Cu(In,Ga)Se_2$-based thin film solar cells*, Thin Solid Films, vols.480–481, pp.118– 123, 2005.

[37] M. Rusu, M. Bär, S. Lehmann, S. Sadewasser, L. Weinhardt, C. A. Kaufmann, E. Strub, J. Röhrich, W. Bohne, I. Lauermann, Ch. Jung, C. Heske, and M. Ch. Lux-Steiner, "*Three-dimensional structure of the buffer/absorber interface in $CdS/CuGaSe_2$ based thin film solar cells*," Applied Physics Letters, vol. 95, pp. 173502-1-173502-3, 2009.

[38] J. Kiss, T. Gruhn, G. Roma, and C. Felser, *Theoretical Study on the Diffusion Mechanism of Cd in the Cu-Poor Phase of $CuInSe_2$ Solar Cell Material*, J. Phys. Chem. C, vol. 117, pp. 25933−25938, 2013.

[39] C. Platzer-Björkman, P. Zabierowski, J. Pettersson, T. Törndahl, M. Edoff, *Improved fill factor and open circuit voltage by crystalline selenium at the $Cu(In,Ga)Se_2$/buffer layer interface in thin film solar cells*, Progress in Photovoltaics: Research and Applications, vol.18, pp.249–256, 2010.

[40] Y. Yan, R. Noufi, K. M. Jones, K. Ramanathan, M. M. Al-Jassim, and B. J. Stanbery, *Chemical fluctuation-induced nanodomains in $Cu(In,Ga)Se_2$ films*, Applied Physics Letters, vol. 87, pp. 121904-1-121904-3, 2005.

[41] K. Ramanathan, H. Wiesner, S. Asher, D. Niles, J. Webb, J. Keane, R. Noufi, "*Thin-Film Structures for Photovoltaics,"* Materials Research Society Symposia Proceedings no. 485, Pittsburgh, 1998, pp. 121–126.

[42] J.-F. Guillemoles, L. Kronik, D. Cahen, U. Rau, A. Jasenek, and H.-W. Schock, "*Stability Issues of $Cu(In,Ga)Se_2$-Based Solar Cells*," The Journal of Physical Chemistry B, vol. 104, pp. 4849-4862, 2000.

[43] X. He, P. Ercius, J. Bailey, G. Zapalac, N. Mackie, A. Bayman, J. Varley, V. Lordi, and Angus Rockett, *Cu rich domains and secondary phases in PVD-CdS / PVD-$CuIn_{1-x}Ga_xSe_2$ heterojunctions*, Photovoltaic Specialists Conference (PVSC), 2012 38th IEEE, 3-8 June 2012.

[44] X. Q. He, G. Brown, K. Demirkan, N. Mackie, V. Lordi, and A. Rockett, Microstructural and Chemical Investigation of PVD-CdS/PVD-$CuIn_{1-}$

$_xGa_xSe_2$ Heterojunctions: A Transmission Electron Microscopy Study,
IEEE Journal of Photovoltaics, vol. 4, no. 6, pp. 1625-1629, 2014.